EDINBURGH INSTRUMENTS

Multimodal Imaging

Raman and Beyond

eBook Series

edinst.com

Contents

Multimodal Raman, Photoluminescence & Imaging of CVD Grown WSe_2

Key Highlights

- Multimodal imaging using one instrument and one software package to fully characterise layer-dependent optoelectronic properties.
- Raman Imaging.
- Photoluminescence Imaging.
- Second Harmonic Generation Imaging.

Multimodal Raman, Photoluminescence & SHG Imaging of CVD Grown WSe_2

Two-dimensional transition-metal dichalcogenides are a class of layered semiconducting materials that exhibit unique layer-number-dependent optical and electronic properties. In this application note, we will discuss how the RMS1000 Confocal Mircoscope enables multimodal imaging of tungsten diselenide (WSe_2), with five multimodal imaging options: reflected brightfield & darkfield, Raman, photoluminescence and second harmonic generation to fully characterise its layer-dependent optoelectronic properties.

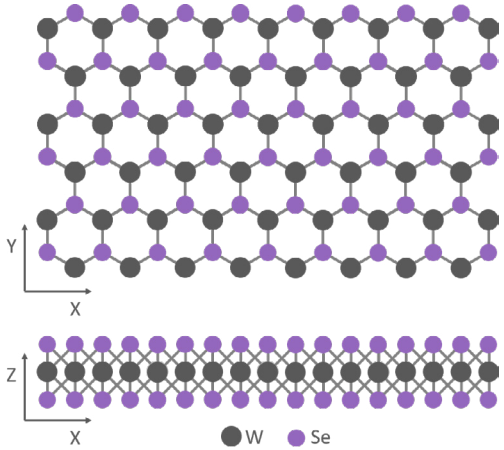

Figure 1: Monolayer WSe_2 Crystal Structure.

Materials & Methods

WSe_2 crystals were grown on a Si substrate using chemical vapour deposition (CVD) and characterised using an Edinburgh Instruments RMS1000 Confocal Microscope. The RMS1000 was equipped with a 100x NA 0.9 objective and a back-illuminated CCD camera. For Raman and photoluminescence imaging, the WSe_2 was excited with a 532 nm laser using a 1800 gr/mm and 300 gr/mm diffraction grating to acquire the Raman and photoluminescence spectra respectively. For second harmonic generation (SHG) imaging, a Chromacity 1040 HP femtosecond fibre laser (Chromacity Ltd. UK) operating at 1040 nm and 80 MHz was coupled to the RMS1000 for excitation, and the SHG response was acquired using a 300 gr/mm diffraction grating.

Figure 2: Edinburgh Instruments RMS1000 Multimodal Confocal Microscope.

Reflected Brightfield and Darkfield Imaging

The WSe_2 crystal was first widefield imaged using reflected brightfield and darkfield (Figure 3). In the reflected brightfield image, the reflective silicon substrate appears bright and the absorbing WSe_2 crystal deposited atop is darker. Nucleation sites appear as dark spots across the crystal surface, as well as a stronger absorbing domain in the centre that is suggestive of multilayer WSe_2.

Reflected darkfield imaging provides complementary information. In darkfield, the sample is illuminated at an oblique angle and steps in sample surface height cause increased scattering and appear bright in the image. The darkfield image reveals there are two regions in the central domain with different heights, likely due to different WSe_2 layer numbers.

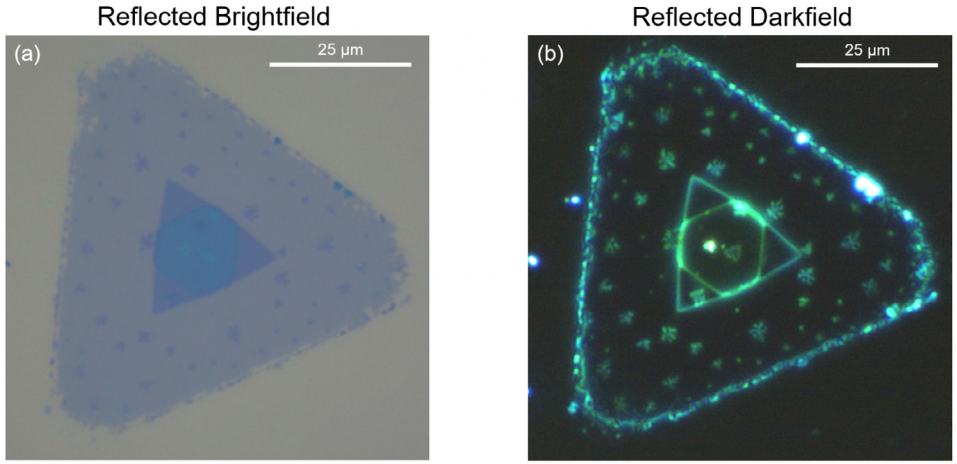

Figure 3: (a) Reflected brightfield and (b) reflected darkfield imaging of the WSe_2 crystal.

Raman Imaging

The crystal was next Raman imaged (Figure 4). WSe_2 has a characteristic Raman peak at 250 cm^{-1} (Figure 4d) which corresponds to the in-plane E^1_{2g} and out-of-plane A_{1g} phonon modes of WSe_2. In contrast to other transition-metal dichalcogenides, the E^1_{2g} & A_{1g} phonon modes are almost degenerate in WSe_2 and are not individually resolved, with both contributing to the 250 cm^{-1} peak.[1,2] In the centre of the crystal, an additional peak at 310 cm^{-1} is observed (marked with arrows in Figure 4d). This peak is symmetry forbidden in monolayer WSe_2 and indicative of multilayer WSe_2.[2]

The E^1_{2g} / A_{1g} peak intensity (Figure 4a) is highest in the large primary triangle domain, and reduces by ~80% within the inner triangle domain. The reduction in E^1_{2g} / A_{1g} intensity is indicative of a change from monolayer to multilayer WSe_2.[1] The E^1_{2g} / A_{1g} peak position (Figure 4b) shifts from 250 cm^{-1} in the primary domain to 247 cm^{-1} within the inner domain which supports a change in layer number.[3] The E^1_{2g} / A_{1g} peak also shifts towards higher wavenumbers at the edges of the crystal which is attributed to changes in the local microenvironment at the disordered edges.

Ramacle® spectral matching analysis (Figure 4c) identified three distinct Raman spectral regions in the crystal. In spectral matching, spectra at user-selected locations in the map are designated as archetypes and the deviation of all other spectra in the map from the archetype is calculated. Lower deviations from the archetype spectra are represented by more intense colour. The monolayer WSe_2 primary domain is highlighted in blue while the inner domain was found to be composed of two regions (highlighted in red and green) with subtly different E^1_{2g} / A_{1g} Raman peak shapes. This agrees with the change in surface height in the inner domain observed in the darkfield image.

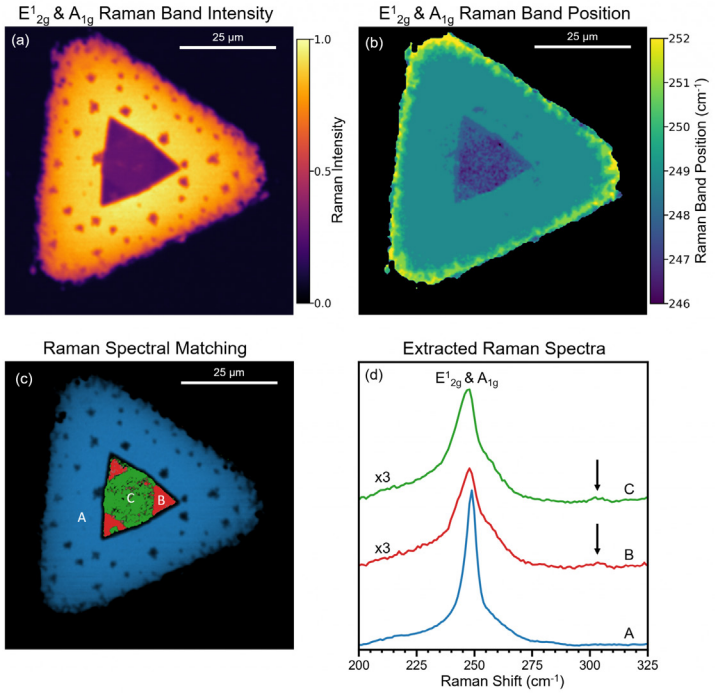

Figure 4: Raman imaging of WSe_2. (a) Intensity of the E^1_{2g} / A_{1g} (250 cm^{-1}) Raman band, (b) peak position of the E^1_{2g} / A_{1g} Raman band, (c) least squares spectral matching revealing three distinct Raman spectral areas, (d) averaged Raman spectra from areas A, B and C; spectra B and C are scaled in intensity by a factor of three and the arrows mark the location of the multilayer 310 cm^{-1} peak. The Raman imaging parameters were: 40 x 40 μm^2, 200 x 200 pixels, 50 ms integration time, 532 nm laser, 1800 gr/mm diffraction grating, 300 µm pinhole.

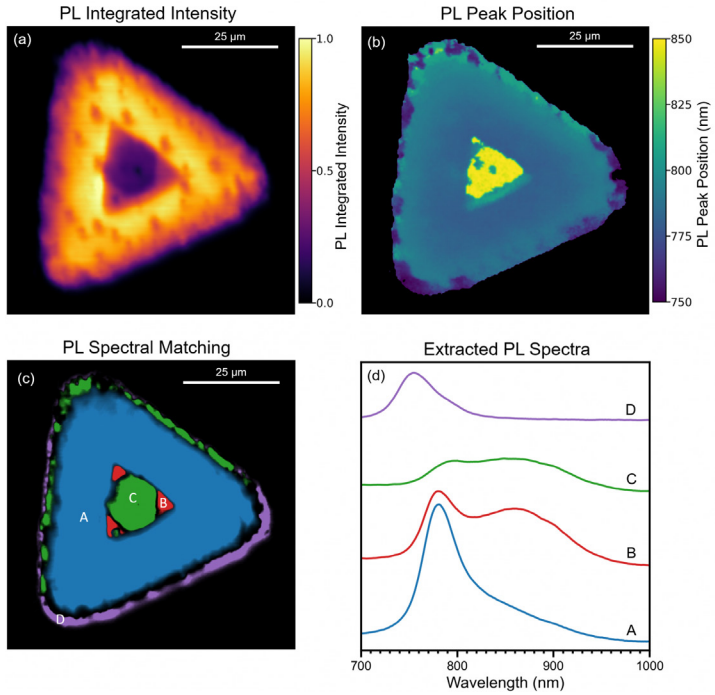

Figure 5: Photoluminescence imaging of WSe_2. (a) Integrated intensity of the PL response, (b) PL primary peak position, (c) least squares spectral matching revealing four distinct PL spectral areas, (d) averaged PL spectra from areas A, B, C and D. The PL imaging parameters were: 40 x 40 μm^2, 200 x 200 pixels, 30 ms integration time, 532 nm laser, 300 gr/mm diffraction grating, 300 µm pinhole.

Photoluminescence Imaging

To obtain additional insight into the inner domain, the crystal was photoluminescence (PL) imaged (Figure 5). The total PL intensity (Figure 5a) is lower within the inner domain, and the PL peak position (Figure 5b) red-shifted. Spectral matching (Figure 5c) identified four distinct PL spectral regions across the crystal and their corresponding spectra are shown in Figure 5d.

Region A (blue) is monolayer WSe_2 with PL peak at 780 nm from confined exciton emission. In region B the total PL intensity is decreased with a longer wavelength shoulder peak at 870 nm, while in region C the PL intensity decreases further and spectral weight shifts to the long wavelength shoulder. It has been established that as the number of layers increases in WSe_2, the PL emission red-shifts from exciton based emission at ~1.6 eV (~780 nm) in the monolayer to indirect bandgap emission at ~1.2 eV (~1000 nm) in bulk WSe_2.[1] Region B and C are therefore assigned as bilayer and trilayer WSe_2 respectively. Similarly to the Raman image, significant edge effects were also observed in the PL, with the PL peak position blue-shifted on the lower edge (spectrum D) and red-shifted on the upper edge of the crystal.

Second Harmonic Generation Imaging

To determine the layer orientation within the three identified domains, the crystal was imaged using second harmonic generation (SHG) (Figure 6). SHG imaging is highly sensitive to the crystalline symmetry of transition metal dichalcogenides, with SHG only occurring when there is a non-centrosymmetry in the excitation focal volume. Monolayer WSe_2 is non-centrosymmetric and region A has a measurable SHG response as expected. The symmetry of multilayer WSe_2 depends on the type of layer stacking, 2H or 3R.[5] In 3R stacking, each layer has the same orientation and the multilayer is non-centrosymmetric with SHG response increasing with layer number. In contrast, in 2H stacking, each layer is rotated 180° with respect to the adjacent layers and odd-numbered multilayers are net non-centrosymmetric with an SHG response similar to the monolayer while even-numbered multilayers are net centrosymmetric with no SHG response.[4,5]

The bilayer WSe_2 in region B has an SHG response that is twice that of the monolayer, and the two layers therefore must be 3R stacked. The trilayer WSe_2 in region C has diminished SHG response compared to the monolayer which indicates the third layer in the trilayer is rotated relative to the first and second layers resulting in a partial restoration of centrosymmetry. The blue, red and green dashed triangles in Figure 6a illustrate the relative orientations of the three layers in the crystal. The growth of the third layer (green) has terminated at the boundaries of the second layer (red) resulting in a partial triangle.

Conclusion

Through a combination of widefield, Raman, PL and SHG imaging techniques, the layer number and stacking type in a CVD-grown WSe_2 crystal was identified. The multimodal imaging capabilities of the RMS1000 Confocal Microscope make it an ideal imaging platform for studying the optoelectronic properties of transition-metal dichalcogenides.

References

1. Todddorf *et al.*, Photoluminescence emission and Raman response of monolayer MoS_2, $MoSe_2$, and WSe_2, *Express*, 2013, 21, 4908-4916
2. Ribeiro-Soares *et al.*, Second Harmonic Generation in WSe_2, *2D Mater.*, 2015, 2, 045015
3. Terrones *et al.*, New First Order Raman-active Modes in Few Layered Transition Metal Dichalcogenides, *Rep.*, 2014, 4, 4215
4. Zhao *et al.*, Atomically phase-matched second-harmonic generation in a 2D crystal, *Light Sci. Appl.*, 2016, 5, e16131
5. Shinde *et al.* Stacking-controllable interlayer coupling and symmetric configuration of multilayered MoS_2, *NPG Asia Mater.*, 2018, 10, e468

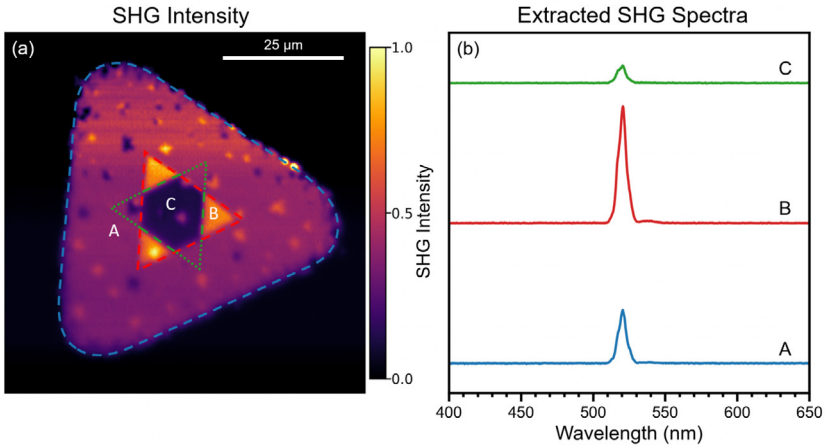

Figure 6: Second Harmonic Generation imaging of WSe_2. (a) Intensity of the SHG peak at 520 nm. (b) extracted SHG response from areas A, B, and C. The SHG imaging parameters were: 40 x 40 µm², 200 x 200 pixels, 11 ms integration time, 1040 nm femtosecond pulsed laser, 300 gr/mm diffraction grating, 300 µm pinhole.

Photoluminescence and Electroluminescence Confocal Imaging of an OLED

Key Highlights

- The optoelectronic properties of an OLED are imaged.
- PL and EL Spectral Imaging.
- PL & EL Lifetime Imaging.

Photoluminescence and Electroluminescence Confocal Imaging of an OLED

In recent years organic light-emitting diodes (OLEDs) have become one of the leading technologies for full-colour display panels in high-end smartphones and televisions.[1] This rapid growth in use has occurred because OLEDs offer an all-around superior performance to liquid crystal displays (LCDs). For example, they are thinner, lighter, more flexible, less power consumptive, and brighter.[2]

In a typical OLED device, electrons and holes are injected into organic electron and hole transport layers and they then recombine in a central doped emission layer. The energy generated from this recombination is transferred to a dopant molecule via resonant transfer, and this causes it to emit light. The colour of the OLED emission is governed by the chemical structure of the dopant molecule in the emission layer. When new OLEDs are developed, the optoelectronic properties of individual components and the complete device can be characterised using photoluminescence (PL) and electroluminescence (EL) spectroscopy.

In this Application Note, the RMS1000 Confocal Raman Microscope is used to characterise and spatially resolve the optoelectronic properties of a fabricated OLED device with four imaging modalities: PL, EL, time-resolved PL (TRPL), and time-resolved EL (TREL). Using a confocal microscope to characterise an OLED's spectral and time-resolved properties provides much greater detail than bulk measurements.

Materials and Methods

A phosphorescent OLED device was fabricated via vacuum sublimation using $Ir(MDQ)_2(acac)$ as the dopant and encapsulated with a glass coverslip and optical epoxy to prevent degradation. The sample was placed on an electrical probe stage (LINKAM HFS350EV-PB4) and two tungsten probes were connected to the electrodes on the device to illuminate a single OLED pixel. Spectral and time-resolved PL and EL imaging were performed using an RMS1000 Confocal Raman Microscope, Figure 1.

The electrical probe stage containing the sample was placed in the microscope stage insert, Figure 2. For spectral PL measurements, the system was equipped with a 532 nm CW laser and a back-illuminated CCD camera. For TRPL measurements, the system was equipped with an externally coupled EPL-405 picosecond pulsed diode laser, phosphorescence lifetime electronics based on single photon counting multichannel scaling (MCS), and a High-Speed PMT lifetime detector.

For spectral EL measurements, a Keithley 2450 Source Measurement Unit (SMU) was used to apply a bias to the OLED device and electroluminescence detected with the CCD. Finally, for TREL measurements, a Tektronix 31102 Arbitrary Function Generator (AFG) was used to apply a train of short voltage pulses to the OLED. The resulting decay after each pulse was measured using MCS.

Results and Discussion

Large Area Photoluminescence and Electroluminescence Spectral Imaging

The OLED was first investigated using a combination of spectral PL and EL. When combined with imaging using a confocal microscope, these techniques can reveal information about the distribution of the optically relevant materials throughout the device and the device's overall quality in terms of the uniformity of the emission intensity and colour. The PL image and corresponding spectra in Figure 3 provide information about the distribution of the emissive layer throughout a 4-pixel area on the device, and the location of the electrodes are also shown for reference.

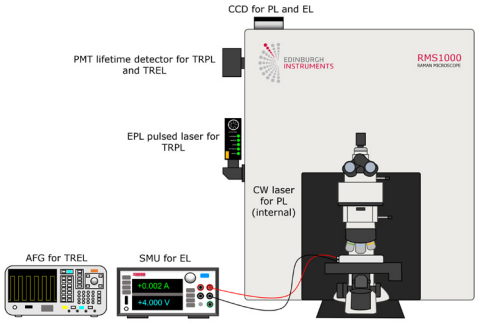

Figure 1: Experimental setup for PL, TRPL, EL, and TREL imaging.

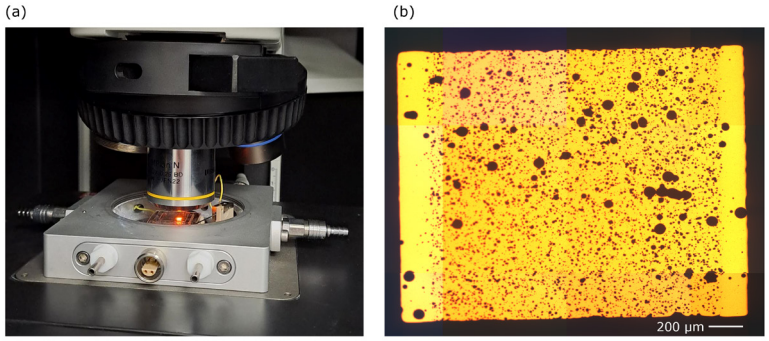

Figure 2: (a) Electrical probe stage fitted on the RMS1000. (b) Widefield view of electroluminescent OLED pixel through the microscope.

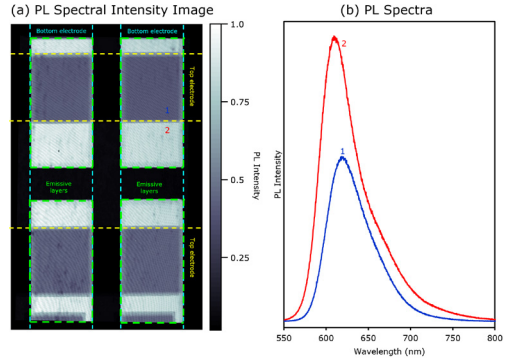

Figure 3: (a) Spectral PL image of OLED device. (b) PL spectra from points 1 and 2 labelled in the image in (a).

The white (highest) and grey (reduced) PL intensity regions, bordered collectively in green, show the location of the organic emissive layers in the four pixels. The grey regions were determined to be the locations at which the emissive layer were covered by the top electrodes. This is because, where the top electrode crosses the emissive layer, the PL emission is reduced to less than half the intensity of the uncovered areas. This is due to the top electrode material attenuating both the incoming laser intensity and the outgoing PL intensity.For EL imaging, the probes were connected to electrodes that intersected on Pixel 2. The resulting EL image and corresponding spectra in Figure 4 reflect this, with EL emission occurring only in the region where the emissive layer in Pixel 2 overlapped with the top and bottom electrodes. With PL mapping, the spatial resolution is predominantly determined by the laser spot size on the sample. In the EL image, there is no excitation laser to give spatial resolution. Instead, for EL, the confocal pinhole diameter was used to provide the spatial resolution by reducing the pinhole diameter to the smallest available setting of 25 µm.

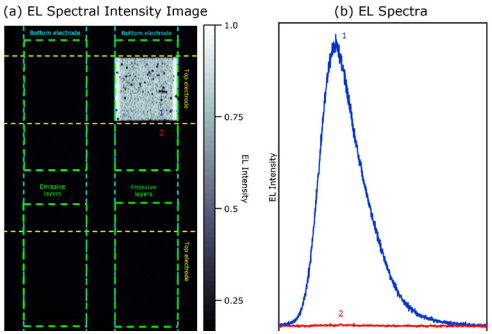

Figure 4: (a) Spectral EL image of OLED device. (b) EL spectra from points 1 and 2 labelled in the image in (a).

The EL intensity is not uniform across the active pixel, which has implications for the quality of the device. There are two vertical strips at the outer edges (white) of the emitting pixel that produces more EL than the rest of the pixel. Furthermore, there are many non-emissive regions in the pixel where the EL intensity is reduced. This indicates defects in the pixel as ideally, an OLED would exhibit intense and uniform emissions across each pixel.

High-Resolution Photoluminescence and Electroluminescence Spectral Imaging

To further investigate the effects seen in the PL and EL maps in the previous section, a smaller region on the EL active pixel, Figure 5a and b, was imaged using PL and EL. The upper region within the mapping grid was where the emissive layer overlapped with the electrodes, and the lower region was the emissive layer alone. The PL intensity image, Figure 5c, again shows that the top electrode attenuates the incoming laser and outgoing PL light, because the intensity from the electrode covered emissive layer is less than the uncovered emissive layer. The PL peak wavelength image, Figure 5d, shows that within the EL active electrode covered emissive layer, the PL emission is red-shifted (620 nm) compared to the uncovered emissive layer region (611 nm). This change in peak wavelength indicates that different energy levels are being accessed in the different regions.

The EL imaging shows that the less emissive defects in the pixel, Figure 5e, have a large redshift, Figure 5f, compared to the rest of the pixel. This is caused by the decrease in intensity of the EL band seen across the rest of the pixel, and the simultaneous increase in a second, lower energy EL band at 662 nm. Additionally, in the region at the very bottom of the EL active region in Figure 5, a blue shift occurs, which is consistent with the wavelength change seen across the PL image. All of these observations from high-resolution spectral imaging reveal a much greater level of complexity than would be detected with bulk PL and EL measurements of the complete OLED device.

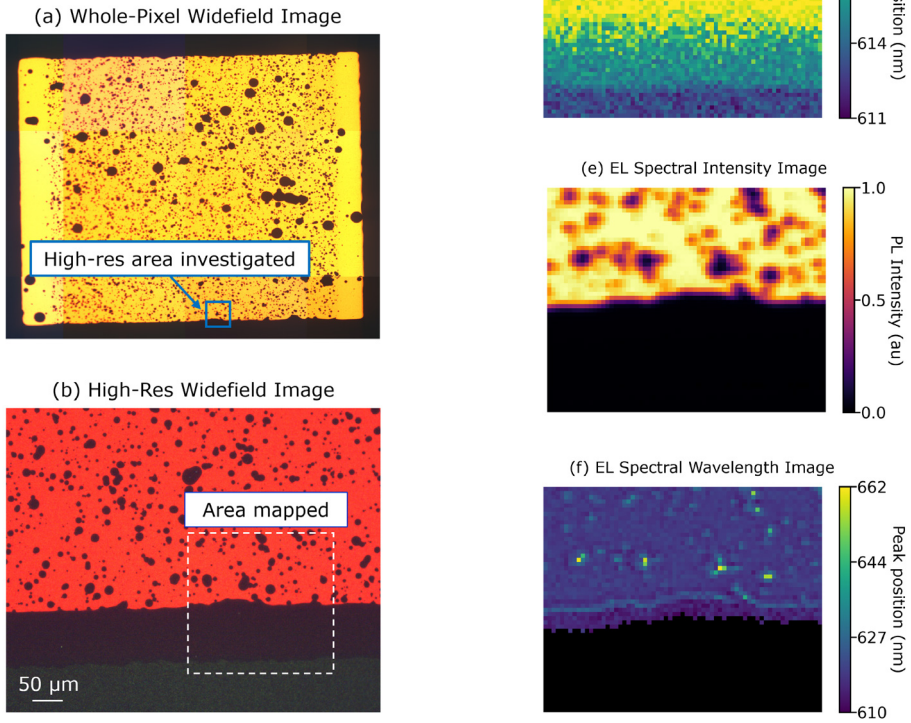

Figure 5: (a) Whole-pixel and (b) high-resolution widefield images of electroluminescent OLED pixel. (c) PL intensity and (d) peak wavelength images of the EL boundary of the OLED pixel. (e) EL intensity and (f) peak wavelength images of the same area.

High-Resolution Time-Resolved Photoluminescence and Electroluminescence Imaging

To obtain additional information TRPL and TREL imaging were performed on the same area, Figure 6. Here, the sample was subject to laser and electrical pulses for PL and EL, respectively and PL and EL lifetime decays of the OLED were recorded at 614 nm in MCS mode. The decays were fit with a single exponential decay model to extract the lifetime.

In the TRPL image in Figure 6a, the PL lifetime within the EL active region (upper region) was approximately 200 ns shorter than the PL lifetime in the EL inactive region (lower region).
The longest and shortest lifetimes recorded were 800 ns and 600 ns, respectively, Figure 6b. A similar gradient was observed here to the PL intensity and wavelength images in Figure 5, where the emission became less intense going down the map and a blue shift occurred. Therefore, the TRPL data supports the conclusion that different energy levels are being accessed across the dopant strip when excited optically. In the TREL image in Figure 6b, the lifetime is similar across the entire region, approximately 470 ns.
The EL lifetime was found to be significantly shorter than PL lifetime recorded within the same area.

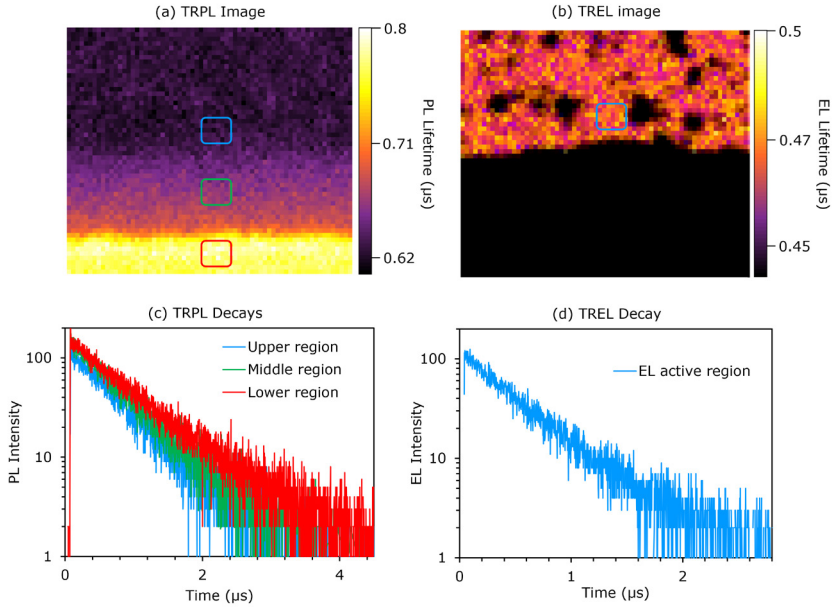

Figure 6: (a) Time-resolved PL image of OLED pixel. (b) Time-resolved EL image of OLED pixel. (c) PL lifetime decays from the image in (a). (d) EL lifetime decay from the image in (b).

Conclusion

In this Application Note, the RMS1000 Confocal Raman Microscope was used to perform PL, EL, TRPL, and TREL imaging of an OLED device. Combined, these various imaging modes provided detailed information about the location of the emissive layer and electrodes throughout the device; the efficiency and colour uniformity of a pixel within the device under working conditions; and relative information about the energy levels being accessed by the two processes.

References

1. A. Salehi et al., Recent Advances in OLED Optical Design, Adv. Funct. Mater., 2019, 29, 1808803, DOI: 10.1002/adfm.201808803.
2. J. M. Ha et al., Recent Advances in Organic Luminescent Materials with Narrowband Emission, NPG Asia Mater., 2021, 13, 1–36, DOI: 10.1038/s41427-021-00318-8.

Multiphoton Imaging of Mouse Intestine

Key Highlights

- Two-photon techniques to study biological samples: 2PEF & SHG.
- Femtosecond laser and CCD camera for spectral 2PEF & SHG.
- Femtosecond laser with pulse picker, TCSPC electronics, and hybrid photodetector for 2PEF lifetime.

Multiphoton Imaging of Mouse Intestine

Two-photon excited fluorescence (2PEF) and second harmonic generation (SHG) are complementary multiphoton imaging techniques for studying biological samples. Both imaging techniques utilise femtosecond pulsed infrared excitation light to generate shorter wavelength light to image the sample but operate via fundamentally different physical processes (Figure 1). In 2PEF, two infrared photons are simultaneously absorbed by a fluorophore promoting it to an excited state which then radiatively relaxes emitting shorter wavelength fluorescence.

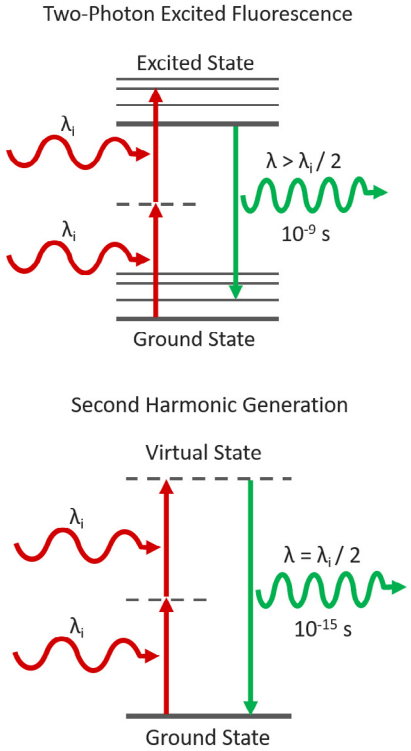

Figure 1: Two-Photon Excited Fluorescence vs Second Harmonic Generation.

In contrast, SHG is not an absorption and emission process and instead the two infrared photons combine in a non-linear optical material with a particular symmetry to generate a new photon with exactly half the wavelength of the incident photons. Both techniques take advantage of the lower scattering and absorption of infrared light to enable imaging deep into tissue. In this application note, an Edinburgh Instruments RMS1000 Confocal Raman Microscope is used to image a tissue section of mouse intestine using 2PEF and SHG microscopy.

Experimental Configuration

The sample to be imaged was a section of mouse intestine tissue stained with Alexa Fluor® 568. The RMS1000 was equipped with a motorised XYZ stage and a 40x NA = 0.75 objective. For spectral imaging the RMS1000 was equipped with a back-illuminated CCD camera and for lifetime imaging; a photon counting Hybrid Photodetector and time-correlated single photon counting (TCSPC) electronics. 2PEF and SHG both require a very high excitation intensity, which is achieved using a mode-locked femtosecond pulsed laser. The RMS1000 has external laser coupling ports that enable the optical coupling of femtosecond lasers into the microscope. The optical setup for the femtosecond excitation source is shown in Figure 2. The laser was a Chromacity 1040 HP femtosecond fibre laser with an output wavelength of 1040 nm and an 80 MHz repetition rate (Chromacity Ltd., UK). For lifetime imaging the output of the laser was pulse picked to the desired pulse frequency using a pulseSelect pulse picker (APE GmbH, Germany). A small fraction of the pulse picker output was picked-off into an Edinburgh Instruments OT900 optical trigger module to trigger the TCSPC electronics. For spectral measurements, the pulse picker was bypassed, and the 80 MHz laser output coupled directly into the RMS1000.

2PEF & SHG Spectral Imaging with CCD Camera

The intestine tissue section was first imaged spectrally using the CCD camera of the RMS1000. A 900 µm x 800 µm area of the sample was mapped with a spatial resolution of 2 µm. The sample was excited at 1040 nm 80 MHz and the 2PEF and SHG signals acquired simultaneously using the CCD camera. The resulting multiphoton image is shown in Figure 3a. 2PEF at 630 nm from the Alexa Fluor® 568 dye is shown in teal and reveals the structure of the intestinal villi. The area shown in pink is SHG at 520 nm from fibrillar collagen near the intestinal wall. SHG only occurs from molecular structures that are non-centrosymmetric and fibrillar collagen is a common biological structure with this property, eliciting a strong SHG response. Each point in the image has a corresponding spectrum, and the spectra at two points A and B are shown in Figure 3b. At point A there is only 2PEF from the Alexa Fluor® 568 dye which has a broad emission centred at 630 nm, while at point B there is an additional sharp peak at 520 nm which is the SHG signal. The colour image in Figure 3a was obtained by plotting the intensity of the spectra at 630 nm and 520 nm for 2PEF and SHG respectively.

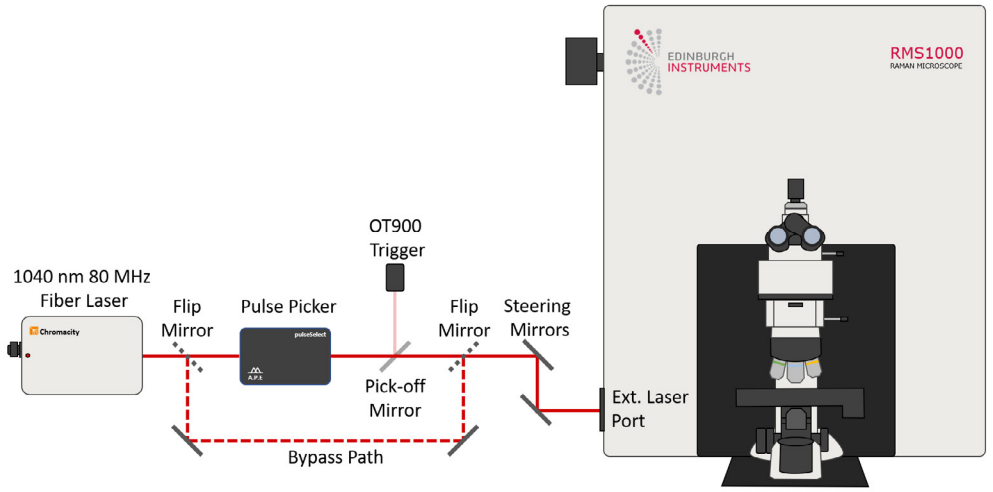

Figure 2: Optical setup for 2PEF and SHG microscopy with the Edinburgh Instruments RMS1000.

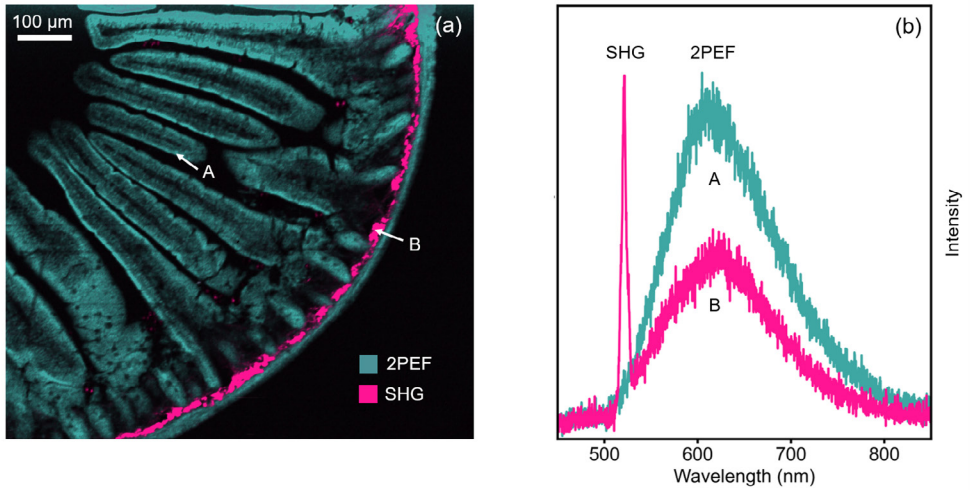

Figure 3: (a) 2PEF and SHG image of mouse intestine section stained with Alexa Fluor® 568 and (b) extracted spectra from two points in the image.

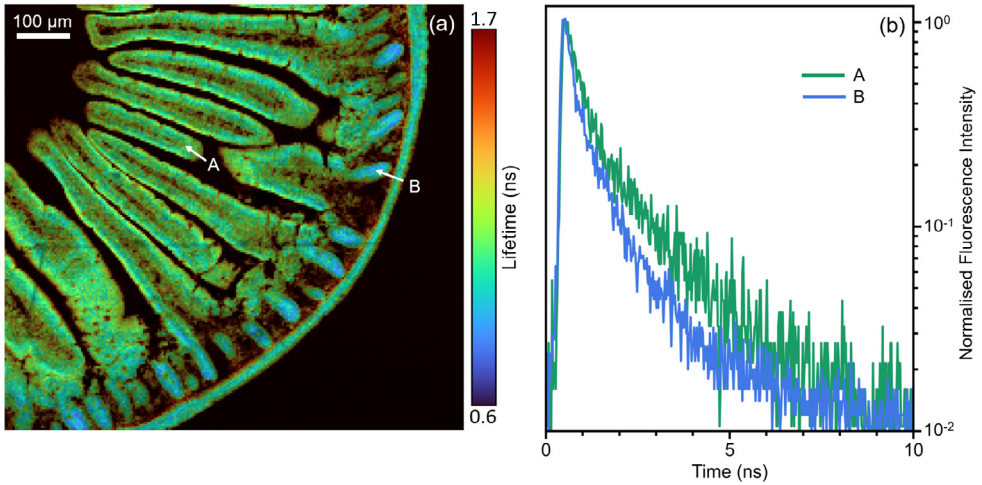

Figure 4: (a) 2PEF lifetime image of mouse intestine section stained with Alexa Fluor® 568 and (b) extracted fluorescence decays from two points in the image.

2PEF Lifetime Imaging with Hybrid Photodetector

Additional information can be obtained by two-photon fluorescence lifetime imaging. For lifetime imaging the repetition rate of the laser was lowered to 20 MHz using the pulse picker to ensure complete fluorescence decay between pulses. The same 900 µm x 800 µm area was mapped and the fluorescence decay at each point recorded using TCSPC on the photon counting Hybrid Photodetector. Each fluorescence decay was fit with an exponential model using the RMS1000 Ramacle® software and the resulting lifetime image is shown in Figure 4a. The lifetime image shows a decreased fluorescence lifetime in the intestinal crypts near the intestinal wall compared with the villi; an example of the increased information that can routinely be obtained from lifetime imaging.

Conclusion

A section of mouse intestine was imaged using multiphoton microscopy with the RMS1000 Confocal Raman microscope. The RMS1000 can be equipped with an external femtosecond laser and TCSPC lifetime electronics for advanced spectral and time-resolved multiphoton imaging techniques such as 2PEF and SHG which augments its core Raman imaging capability.

Raman, Photoluminescence, and PLIM Imaging

Key Highlights

- The RMS1000 Confocal Raman Microscope is capable of both fluorescence (FLIM) and phosphorescence (PLIM) lifetime imaging.
- Raman spectral imaging, PL spectral imaging, and lifetime imaging can be performed on the same sample area to maximise the information gained from a sample.

Raman, Photoluminescence, and PLIM imaging using the RMS1000 Confocal Microscope

In confocal microscopy, it is advantageous to combine multiple complementary spectroscopic techniques to maximise the information generated from a single sample. Two confocal spectroscopic techniques that are widely used are Raman and photoluminescence (PL) imaging, which provide information on the vibrational and electronic energy levels of the sample by reading out wavelength-dependent spectra.[1] Both techniques can be performed on a confocal Raman microscope equipped with a continuous wave (CW) laser and a charge-coupled device (CCD) detector.

Another powerful imaging technique is fluorescence lifetime imaging (FLIM) or phosphorescence lifetime imaging (PLIM). In FLIM/PLIM, the variation in fluorescence or phosphorescence lifetime across a sample is imaged.[2] Lifetime imaging can be used to determine chemical changes in the microenvironment of fluorophores/phosphors, detect conformational changes, and characterise properties like charge carrier efficiency in semiconductor materials and autofluorescence in tissue. Additionally, unlike intensity, the lifetime is independent of fluorophore/phosphor concentration, and it can be used to discriminate between materials that have overlapping emission peaks. Since FLIM/PLIM is a time-resolved method, it requires a pulsed excitation source, a photon-counting lifetime detector, and photon-counting electronics.

This Technical Note demonstrates how the RMS1000 Confocal Raman Microscope can be used to perform Raman, PL, and PLIM imaging of a sample all within a single software package. The integration of these three imaging techniques into the RMS1000 makes it ideal for both the analysis of multiple sample types and dedicated, in-depth studies of single samples.

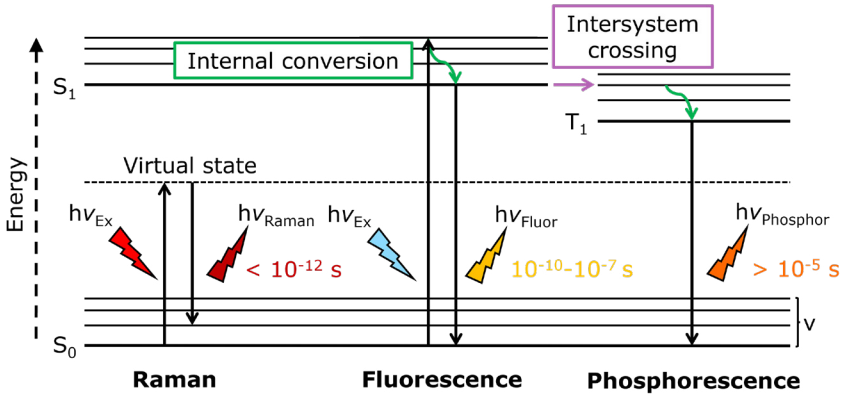

Figure 1: Jablonski diagram showing the energy transitions and relative timeframes of Raman scattering, fluorescence, and phosphorescence.

Materials and Methods

Two photoluminescent rare-earth phosphors with different chemical structures and optical properties were mixed and deposited onto a calcium fluoride disk for spectroscopic imaging. Raman, spectral PL, and PLIM measurements were then performed on microparticles of the two phosphors using an RMS1000 Confocal Raman Microscope, Figure 2.

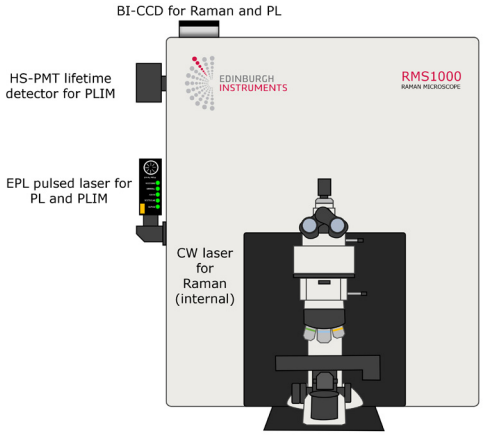

Figure 2: RMS1000 Confocal Raman Microscope setup used for Raman, spectral PL, and FLIM Imaging.

The schematic in Figure 2 shows how the RMS1000 was configured for each imaging mode. For spectral PL and PLIM measurements, an externally coupled HPL-405 picosecond pulsed diode laser was used. For spectral PL the laser was operated at 80 MHz and used as a quasi-CW excitation source and the resulting PL emissions were detected using a back-illuminated charge-coupled device (BI-CCD) camera. For PLIM measurements, the HPL-405 laser was used at 10 kHz along with fluorescence and phosphorescence lifetime electronics capable of time-correlated single photon counting (TCSPC) and multichannel scaling (MCS), and a High-Speed photomultiplier tube (PMT) lifetime detector. For Raman measurements, the system was equipped with an internal 785 nm CW laser and the BI-CCD. The different excitation sources and detectors needed for each mode are summarised in Table 1. The three imaging modes were performed, and the necessary optical components for each mode were selected and changed, using Ramacle® software.

Table 1: Summary of the excitation source and detector needed for each imaging mode.

Imaging mode	Laser	Detector
PL spectral	CW or pulsed (quasi-CW)	CCD
PLIM	Pulsed	PMT
Raman	CW	CCD

Darkfield Microscopy

An area containing microparticles of the two phosphors was identified using darkfield imaging, Figure 3. The particles, labelled phosphor 1 and phosphor 2, were visually distinguishable under the microscope because they produced green and orange PL under white light illumination, respectively. This area of the sample encompassing the two particles was then analysed using PL, PLIM, and Raman.

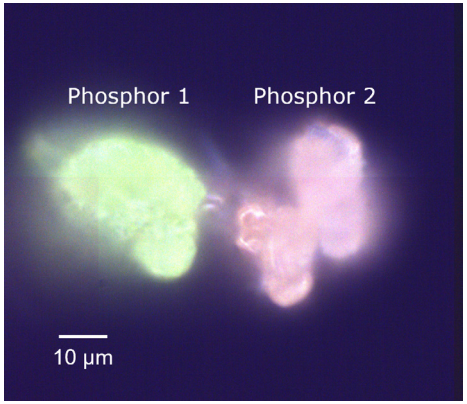

Figure 3: Darkfield image of phosphors 1 and 2.

Photoluminescence

The first spectroscopic technique used to analyse the sample was spectral PL imaging, Figure 4. The PL spectral map shows spectral intensity analyses for phosphors 1 and 2, which had peak emission wavelengths of 549 nm and 640 nm, respectively.

PLIM

Next, PLIM imaging was performed on the sample. Since the two particles produced PL spectra with different emission bands, the wavelength at which the two bands intersected (620 nm) was selected for lifetime measurements. The excitation rate was set to 10 kHz and the electronics module was set to record decays in MCS mode. The PLIM image and corresponding decays in Figure 5 show that the lifetimes of phosphors 1 and 2 were approximately 1.1 µs and 0.7 µs, respectively. Therefore, as well as distinguishing samples by their PL emission wavelengths, the RMS1000 can also be used to discriminate between them by their lifetimes.

Raman

Finally, to discriminate between the two phosphors by their chemical structures, they were imaged using Raman spectroscopy, Figure 6. Since the two phosphors exhibited PL at 549 nm and 640 nm, the 785 nm laser was selected to acquire the Raman image. This ensured that the resulting spectra were free from fluorescent backgrounds.

The Raman image and corresponding spectra in Figure 6 show that the two phosphors exhibited unique vibrational spectra and hence had different chemical structures. The image of phosphors 1 and 2 was built by overlaying the intensity of the Raman bands at 1020 cm^{-1} and 540 cm^{-1}.

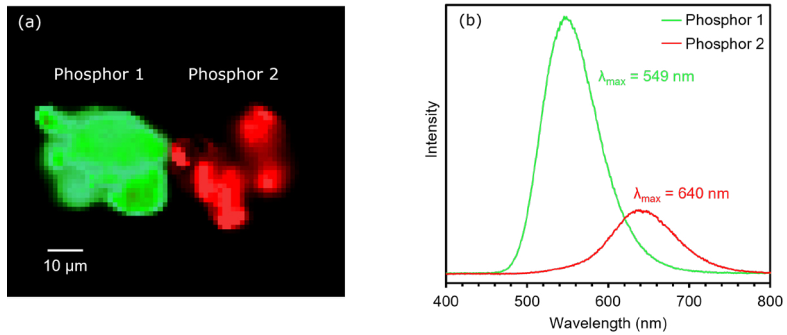

Figure 4: (a) PL image and (b) spectra of phosphors 1 and 2.

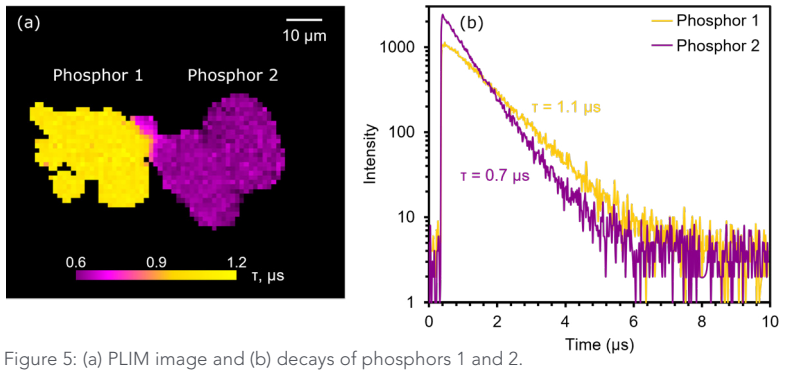

Figure 5: (a) PLIM image and (b) decays of phosphors 1 and 2.

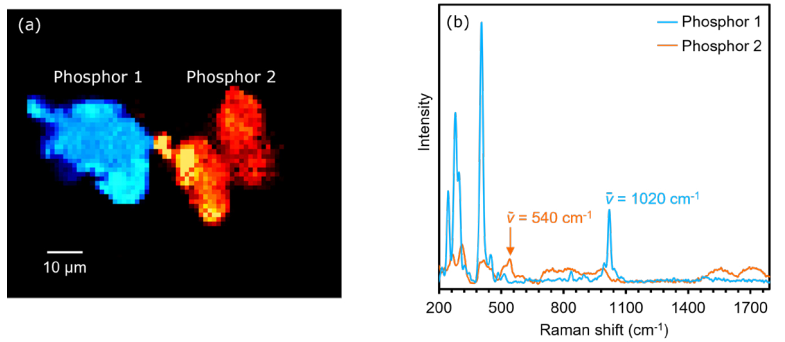

Figure 6: (a) Raman image and (b) spectra of phosphors 1 and 2.

Conclusion

Using the RMS1000 Confocal Raman Microscope, spectral PL, FLIM, and Raman imaging were used sequentially to thoroughly characterise and discriminate between two distinct phosphor microparticles, Figure 7. These techniques provide complementary information and are therefore useful for gaining large amounts of information and a cohesive understanding of samples under investigation.

References

1. I. Pavić et al., Raman and Photoluminescence Spectroscopy with a Variable Spectral Resolution, Sensors (Basel), 2021, 21, 7951, DOI: 10.3390/s21237951.
2. R. Datta et al., Fluorescence lifetime imaging microscopy: fundamentals and advances in instrumentation, analysis, and applications, J. Biomed. Opt., 2020, 25, 071203.

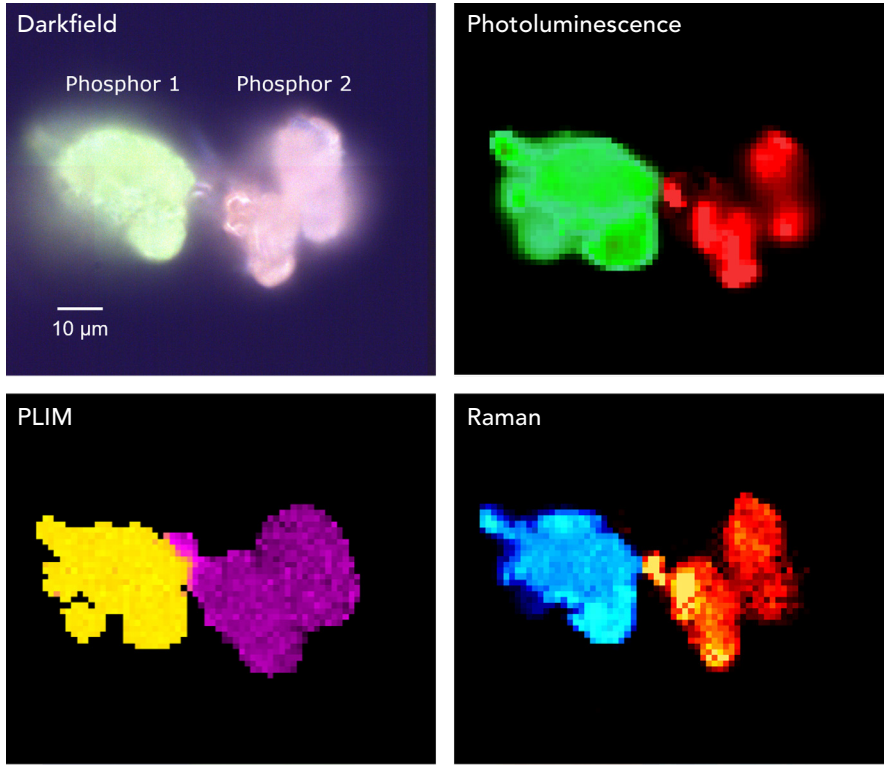

Figure 7: Darkfield, PL, PLIM, and Raman images of phosphor 1 and 2 microparticles.

Photoluminescence in Raman Spectra – Friend or Foe?

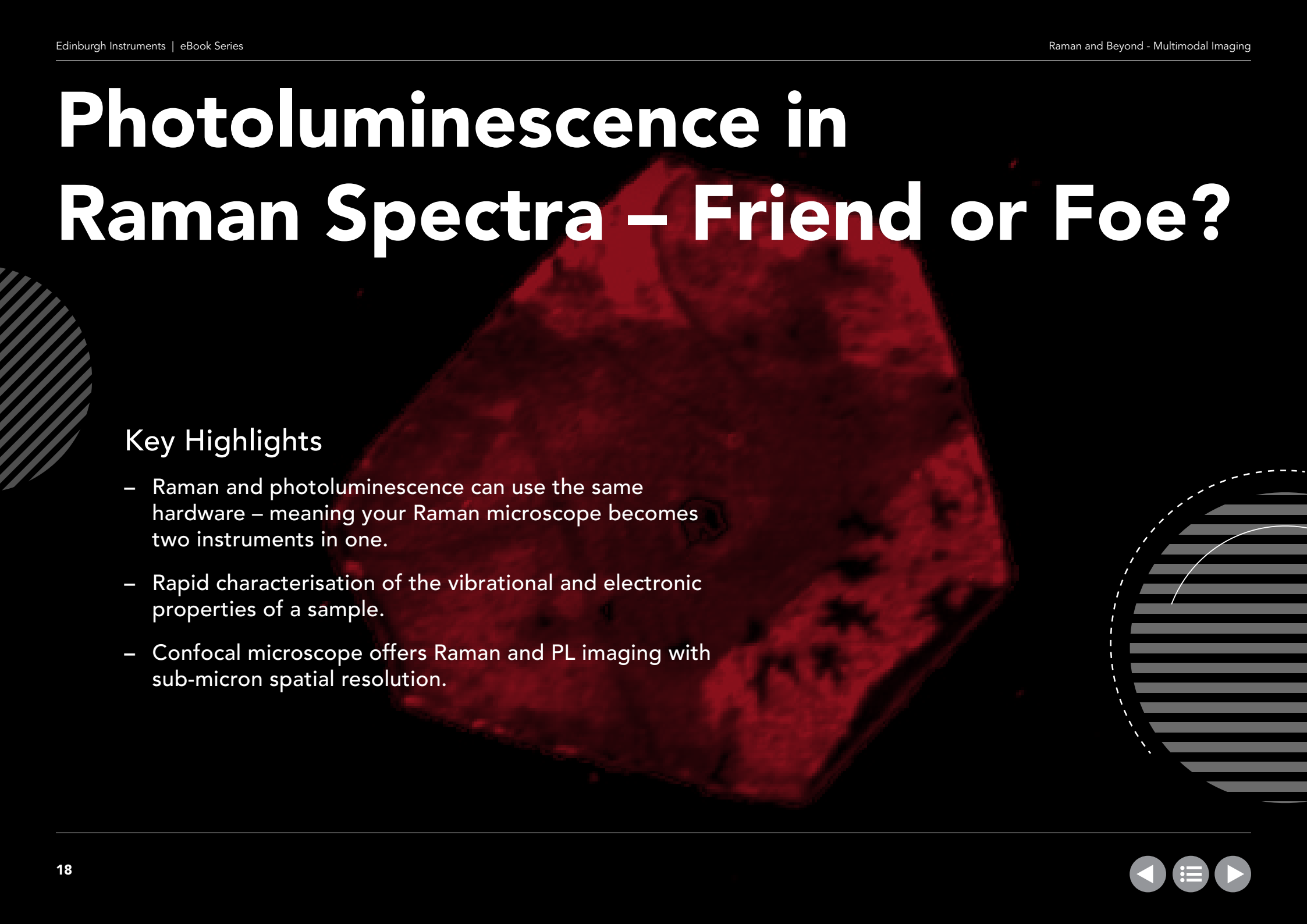

Key Highlights

- Raman and photoluminescence can use the same hardware – meaning your Raman microscope becomes two instruments in one.
- Rapid characterisation of the vibrational and electronic properties of a sample.
- Confocal microscope offers Raman and PL imaging with sub-micron spatial resolution.

Photoluminescence in Raman Spectra – Friend or Foe?

In Raman spectroscopy, photoluminescence (PL), also referred to as fluorescence, is often considered an undesired effect. Strong PL backgrounds can mask Raman peaks making some samples extremely difficult to analyse. Whilst there are numerous ways to help reduce the effect of PL on Raman spectra, in some applications PL can be extremely useful. As a technique, PL spectroscopy can provide electronic information about a sample, which in some cases is not achievable in Raman and is complimentary to the vibrational information from Raman.

This blog highlights when PL and Raman spectroscopy can be used in combination for full sample characterisation. From foe to friend thanks to the wealth of information the two techniques can provide.

2D Materials

2D transition metal dichalcogenides, such as tungsten disulfide (WS_2), are a class of emerging materials with unique optical and electronic properties. Correlative Raman and PL imaging can be used to provide highly detailed information without any sample preparation. In the case of 2D materials, both the Raman and PL information can be captured in one spectrum using the same laser. The Raman peaks occur at the beginning of the spectrum, with the PL occurring enough of a distance away from the Raman so there is no overlap, Figure 1.

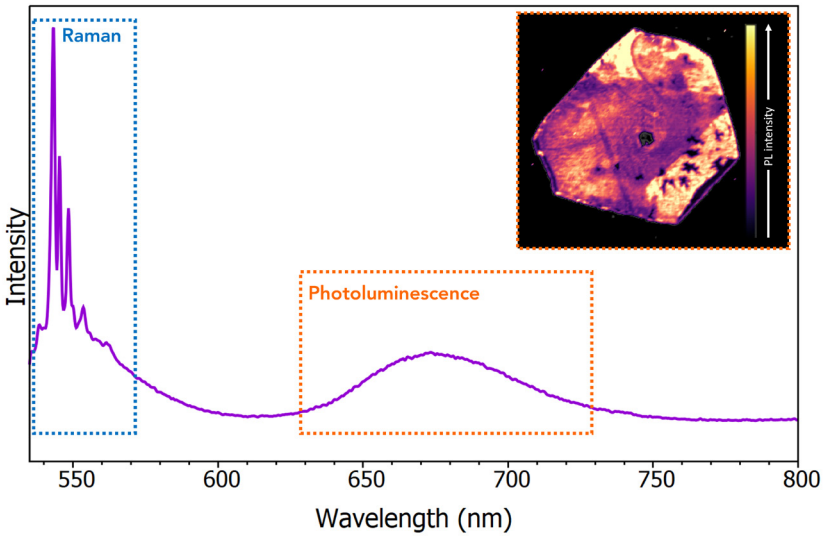

Figure 1: Raman and PL spectrum obtained simultaneously on a WS_2 crystal. Inset shows the false colour PL intensity image of the crystal

The Raman bands can be used for layer number determination and strain evaluation. PL imaging adds further supporting data on layer number plus information on strain, doping, and defects.

Learn more about 2D materials: High-Resolution Raman & PL Imaging of MoS_2

Forensics

In a forensics laboratory, a wide range of samples need to be investigated, but in some instances, these samples will exhibit such significant PL that Raman analysis is not possible. This does not mean the end of the road for the Raman spectrometer though, as the samples may exhibit different PL emissions. For example, in forgery cases, samples are likely to exhibit a high PL response as they contain fluorophores. Figure 2a shows a case of document analysis where the number 8 looks a bit suspicious. Was it always an 8, or has it been tampered with?

To the human eye, even under the microscope, the number 8 looks like it could be genuine and from one ink source. However, the PL map shown in Figure 2b clearly identifies two different ink sources based on their different peak wavelengths. Figure 2c shows the PL spectra extracted from the red and green regions of the map; we can see from the map how the ink represented in green was applied to turn the 3 into an 8 using the difference in PL peak position.

Read the full application note to learn more: Confocal Raman and Photoluminescence Microscopy for Forensic Investigations

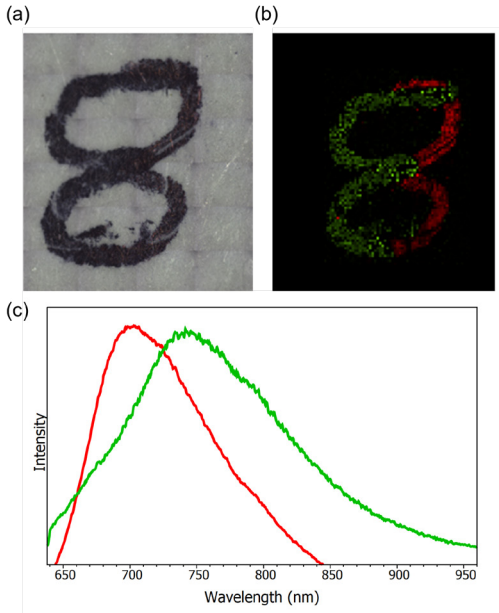

Figure 2: (a) white light image of an ink forgery sample, (b) false coloured PL image revealing 2 inks present in the sample and, (c) PL spectra extracted from the red and green areas of the map.

Geology

Raman and PL can be used together to study geological samples, such as gemstones. They can be used in combination for the identification of the minerals present, as well as any dopants or impurities. One example is corundum, also known as aluminium oxide or alumina (Al_2O_3). Whilst pure corundum is colourless, it is commonly found with transition metal impurities. These impurities make corundum rocks some of the most valuable gems – ruby and sapphire.

Raman can be used to characterise the host Al_2O_3, and the PL is used to identify the transition metal impurities.

For example, chromium impurities create the strong red colour seen in rubies, this has a significant PL response which can easily be identified. Two PL peaks occur at 693.1 nm and 694.5 nm, separated by only 1.4 nm, highlighting the spectral resolution a Raman spectrometer can offer for narrow PL bands, Figure 3. Resolving these peaks is important as their individual positions are indicative of strain in the Al_2O_3 crystal.

Find out how Raman can be used:
Gemstone Identification Using Raman Microscopy

Conclusion

Raman and PL can be both friends and foes, by configuring your system with a range of excitation lasers you can achieve both techniques with no headaches.
This can provide extremely beneficial sample information for a wide range of application areas, be it simultaneous Raman and PL, or sequential.

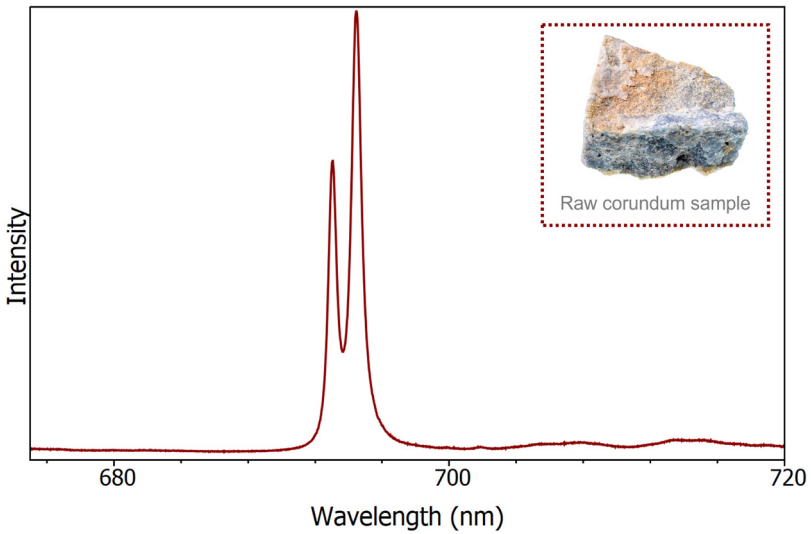

Figure 3: PL spectrum of an Al_2O_3 crystal with Cr^{3+} impurities.

EDINBURGH INSTRUMENTS

edinst.com

STG02 / 08.2023